(12)Indian Patent Application

(21) Application Number: 202241065143

(22) Filing Date: 14/11/2022 (43) Publication Date: 17/05/2024

(71) Applicant(s): L&T TECHNOLOGY SERVICES LIMITED

(72) Inventor(s): Pandey, Indu

(51) International Classifications: H01M 10/0525 G01R 31/392 H01M 4/36 H01M 4/02 A61B 5/00

(54) Title: SELF-REGENERATING LITHIUM-ION BATTERY

(57) Abstract: This disclosure relates to a self-regenerating lithium-ion battery (200). The lithium-ion battery (200) includes a positive electrode (102) and a negative electrode (104). Each of the positive electrode (102) and the negative electrode (104) includes Quantum Nanomaterials (QNs) doped in shape-memory polyurethane (SMPU). The lithium-ion battery (200) further includes a magnetic sensor film coated on each of the positive electrode (102) and the negative electrode (104). The magnetic sensor film monitors a plurality of battery health parameters by monitoring a change in current. The magnetic sensor film includes one-atom-thick film of a plurality of buckled graphdiyne-carbon nitride QNs coated on flexible ceramic fibers. The lithium-ion battery (200) further includes an electrolyte in contact with each of the positive electrode (102) and the negative electrode (104). The electrolyte is configured to rectify one or more anomalies detected based on at least one of the plurality of battery health parameters.

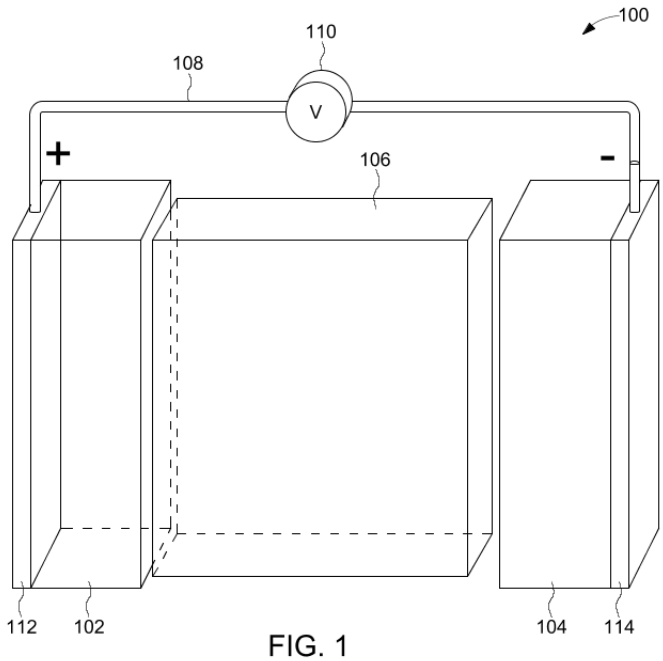

FIG. 1

FORM 2

THE PATENTS ACT 1970
(39 OF 1970)
&
The Patent Rules, 2003

Complete Specification

(See Section 10 and Rule 13)

1. TITLE OF THE INVENTION

SELF-REGENERATING LITHIUM-ION BATTERY

2. APPLICANT(S)

(a) NAME : **L&T TECHNOLOGY SERVICES LIMITED**
(b) NATIONALITY : **INDIAN**
(c) ADDRESS : **DLF IT SEZ Park, 2nd Floor – Block 3**
1/124, Mount Poonamallee Road,
Ramapuram, Chennai – 600 089,
INDIA.

3. PREAMBLE TO THE DESCRIPTION

COMPLETE

The following specification describes the invention and the manner in which it is to be performed

DESCRIPTION

Technical Field

[001] This disclosure relates generally to metal ion batteries, and more particularly to a self-regenerating lithium-ion battery.

Background

[002] In the present global scenario, lithium-ion batteries have proven to be indispensible in powering consumer electronics, Electric Vehicles (EVs), and large-scale smart grids primarily due to ease of recharging and portability. However, such advantages also pose a challenge of diminishing battery life with long-term use. Some of the known causes of such degradation in battery performance are overcharging and overheating. During the course of multiple charging cycles, cracks may be formed on the surface of electrodes and electrolyte of the battery that may eventually develop into fractures. This leads to a reduced current flow and ultimately renders the battery unusable.

[003] In the present state of art, methods of reliably detecting such cracks or other deformations at early stages do not exist. Moreover, conventional electrodes and electrolytes are lacking in self-regeneration capabilities that enable recitification of anomalies. Such capabilities, if incorporated in a lithium-ion battery, may greatly enhance battery performance and battery life in the long run. There is, therefore, a need in the present state of art for lithium-ion batteries capable of detection and self regeneration of electrode and electrolyte anomalies.

SUMMARY

[004] In one embodiment, a lithium-ion battery is disclosed. In one example, the lithium-ion battery may include a positive electrode and a negative electrode. Each of the positive electrode and the negative electrode may include Quantum Nanomaterials (QNs) doped in shape-memory polyurethane (SMPU). The SMPU regenerates using shape-memory effect and disulfide exchange reaction. The lithium-ion battery may further include a magnetic sensor film coated on each of the positive electrode and the negative electrode. The magnetic sensor film may monitor a plurality of battery health parameters by monitoring a change in current. The magnetic sensor film may include one-atom-thick film of a plurality of buckled graphdiyne-carbon nitride QNs coated on flexible ceramic fibers. The lithium-ion battery may further include an electrolyte in contact with each of the positive electrode and the negative

electrode, wherein the electrolyte is configured to rectify one or more anomalies. The one or more anomalies are detected based on at least one of the plurality of battery health parameters. The electrolyte may include at least one of: ethylene carbonate (EC), diethylene carbonate (DEC), and a solution of Gallium-Tin-Barbituric acid (GTB)-Lithium hexafluorophosphate ($LiPF_6$).

[005] In one embodiment, a method of assembling a lithium-ion battery is disclosed. In one example, the method may include electrically coupling a positive electrode with a negative electrode. Each of the positive electrode and the negative electrode may include QNs doped in SMPU. The SMPU regenerates using shape-memory effect and disulfide exchange reaction. The method may further include coating a magnetic sensor film on each of the positive electrode and the negative electrode. The magnetic sensor film may monitor a plurality of health parameters by monitoring a change in current. The method may further include disposing each of the positive electrode and the negative electrode in contact with an electrolyte. The electrolyte may be configured to rectify one or more anomalies. The one or more anomalies may be detected based on at least one of the plurality of battery health parameters. The electrolyte may include at least one of EC, DEC, and a solution of GTB- $LiPF_6$.

[006] In one embodiment, a magnetic sensor film for monitoring a plurality of battery health parameters of an electrode is disclosed. In one example, the magnetic sensor film may include a layer of flexible ceramic fibers. The magnetic sensor film may further include one-atom-thick film of a plurality of buckled graphdiyne-carbon nitride QNs coated on the layer of flexible ceramic fibers using wafer technology. The buckled graphdiyne-carbon nitride QNs may include an imprinted memory provided by molecular imprinting. The one-atom-thick film of the buckled graphdiyne-carbon nitride QNs may be formed using spin coating. The imprinted memory may enable recognition of one or more compounds produced due to one or more anomalies detected based on at least one of the plurality of battery health parameters.

[007] It is to be understood that both the foregoing general description and the following detailed description are exemplary and explanatory only and are not restrictive of the invention, as claimed.

BRIEF DESCRIPTION OF THE DRAWINGS

[008] The accompanying drawings, which are incorporated in and constitute a part of this disclosure, illustrate exemplary embodiments and, together with the description, serve to explain the disclosed principles.

[009] **FIG. 1** illustrates an exemplary lithium-ion battery during discharge where embodiments of the present disclosure may be implemented.

[010] **FIG. 2** illustrates an exemplary self-regenerating lithium-ion battery during discharge, in accordance with some embodiments.

[011] **FIG. 3** illustrates self-regeneration mechanism of an exemplary electrode of a lithium-ion battery, in accordance with some embodiments.

[012] **FIG. 4** illustrates rectification of a crack in an exemplary electrolyte of a lithium-ion battery, in accordance with some embodiments.

[013] **FIG. 5** illustrates a flow diagram of an exemplary method for assembling a self-regenerating lithium-ion battery, in accordance with some embodiments.

[014] **FIG. 6** illustrates Scanning Electron Microscopy (SEM) images depicting self-regeneration of an exemplary electrolyte, in accordance with some embodiments.

[015] **FIG. 7** is a table representing self-regenerating properties of various electrolytes, in accordance with some embodiments.

[016] **FIG. 8** is a graph representing self-regeneration percentages of various electrolytes, in accordance with some embodiments.

DETAILED DESCRIPTION

[017] Exemplary embodiments are described with reference to the accompanying drawings. Wherever convenient, the same reference numbers are used throughout the drawings to refer to the same or like parts. While examples and features of disclosed principles are described herein, modifications, adaptations, and other implementations are possible without departing from the spirit and scope of the disclosed embodiments. It is intended that the following detailed description be considered as exemplary only, with the true scope and spirit being indicated by the following claims.

[018] Referring now to FIG. 1, an exemplary lithium-ion battery 100 during discharge where embodiments of the present disclosure may be implemented is illustrated. The lithium-ion battery 100 may include a positive electrode 102, a negative electrode 104, and a separator 106. The separator 106 may be positioned between the positive electrode 102 and the negative electrode 104 to prevent a physical contact between the two electrodes 102, 104 and in turn prevent occurrence of a short circuit.

[019] The positive electrode 102 may include a lithium metal or a lithium metal compound. The negative electrode 104 may be based on a carbon material (such as, graphene,

graphdiyne, fullerenes, lithiated graphite (LiC_6), etc.). Further, the separator 106 may include a permeable membrane (such as glass fibers).

[020] The positive electrode 102 and the negative electrode 104 may be electrically coupled through an external circuit 108. The lithium-ion battery 100 may be used to supply power to a load device 110 when discharging. The load device 110 may be a consumer electronic device (e.g., a smartphone, a laptop, small and large electrical appliances, wireless headphones, toys, etc.), an Electric Vehicle (EV), or an industrial equipment. The lithium-ion battery 100 may be serially connected or connected in parallel with other similar lithium-ion batteries to produce a greater voltage output and power density if required by the load device 110.

[021] The lithium-ion battery 100 may be in a prismatic battery form, a pouch battery form, a cylindrical battery form, or any other shape that may consistently implement the arrangement of the positive electrode 102, the negative electrode 104, and the separator 106 as shown in the figure. Size and shape of the lithium-ion battery 100 may vary based on a specific application for which the lithium-ion battery 100 may be designed. For example, the size, capacity, and power-output specifications of the lithium-ion battery 100 for use in EVs may be different from those used for powering hand-held consumer electronic devices.

[022] Further, each of the positive electrode 102, the negative electrode 104, and the separator 106 may be disposed in an electrolyte. In some embodiments, the electrolyte may be in form of a semi-solid paste disposed through the separator 106 between the positive electrode 102 and the negative electrode 104. The electrolyte may include a lithium salt (e.g., lithium hexafluorophosphate ($LiPF_6$)) in aqueous state. As will be appreciated, the lithium salt may dissociate into free ions in the aqueous state.

[023] The positive electrode 102 may be configured to oxidize the lithium metal or lithium salt (based on the composition of the positive electrode 102) deposited on surface to generate lithium-ion(s), when the lithium-ion battery 100 is charging. The lithium-ion may be released in the electrolyte. Further, the positive electrode 102 may be configured to reduce lithium-ion in the electrolyte to generate lithium metal or lithium salt when the lithium-ion battery 100 is discharging. The lithium metal/salt may be deposited on surface of the positive electrode 102.

[024] The negative electrode 104 may receive the lithium-ion from the electrolyte to generate lithiated carbon deposition on surface when the lithium-ion battery 100 is charging.

Further, the negative electrode 104 may be configured to oxidize the lithiated carbon to generate free electrons and lithium-ion when the lithium-ion battery 100 is discharging.

[025] Further, the positive electrode 102 may be in contact with a positive-side current collector 112 and the negative electrode 104 may be in contact with a negative-side current collector 114. The positive-side current collector 112 may be composed of aluminum (Al) or any other appropriate electrically conductive material. The negative-side current collector 114 may be composed of copper (Cu) or any other appropriate electrically conductive material. While lithium-ion may be exchanged between the positive electrode 102 and the negative electrode 104 via the electrolyte, the free electrons may be exchanged via the positive-side current collector 112 and the negative-side current collector 114. Thus, when the lithium-ion battery 100 is discharging, the free electrons may flow from the negative electrode 104 to the positive electrode 102. Consequently, the free electrons generated may generate an electric current through the external circuit 108. The negative electrode 104 may be used in electrochemical cells such as a photovoltaic cell, a piezoelectric cell, or a pyroelectric cell.

[026] During a course of multiple charging-discharging cycles, the lithium-ion battery 100 may undergo performance degradation (e.g., increase in charging time, decrease in battery life, etc.) over time. The performance degradation may be caused by development of one or more anomalies (such as, cracks and fractures) in at least one of the positive electrode 102, the negative electrode 104, and the electrolyte of the lithium-ion battery 100. Cracks and fractures may also appear due to overcharging or overheating.

[027] Referring now to FIG. 2, an exemplary self-regenerating lithium-ion battery 200 during discharge is illustrated, in accordance with some embodiments. The self-regenerating lithium-ion battery 200 may include the positive electrode 102, the negative electrode 104, and the separator 106, the external circuit 108, the load device 110, the positive-side current collector 112, and the negative-side current collector 114. Further, the positive electrode 102 may be coated with a shape-memory layer 202 and the negative electrode 104 may be coated with a shape-memory layer 204. Each of the shape-memory layers 202 and 204 may include QNs doped in SMPU. The QNs may be silicon QNs or carbon QNs. In an embodiment, size of the QNs may be in a range of about 1 nm to about 5 nm. The SMPU is capable of regenerating using shape-memory effect and disulfide exchange reaction.

[028] In an exemplary scenario, the positive electrode 102 may develop one or more cracks in the surface. In such a scenario, the shape-memory layer 202 may rectify the one or more cracks to regenerate the positive electrode 102 in original or near-original conformation.

Similarly, the shape-memory layer 204 is configured to rectify one or more cracks in the negative electrode 104 using shape-memory effect and disulfide exchange reaction.

[029] Referring now to FIG. 3, self-regeneration mechanism of an exemplary electrode (such as, the positive electrode 102 or the negative electrode 104) of a lithium-ion battery (such as the self-regenerating lithium-ion battery 200) is illustrated, in accordance with some embodiments. In some embodiments, on an electrode surface 302, one or more cracks (such as, a crack 304) may be formed due to overcharging or overheating of the self-regenerating lithium-ion battery 200. It may be noted that the electrode may be composed of silicon QNs or carbon QNs doped in SMPU. Thickness of the QNs may be in range of about 0.3 nm to about 0.5 nm. It may be noted that the QNs may possess quantum properties such as, but not limited to, high resolution, photoluminescence, superposition, or the like, that may enable high performance of the self-regenerating battery 200 in terms of reaction rate and sensitivity.

[030] Further, the SMPU may provide a plurality of sulfur atoms 306. When the crack 304 is formed, the QNs may bring the sulfur atoms closer to each other thereby narrowing the crack 304. Finally, when a sulfur atom is within an optimal distance with respect to another sulfur atom, a disulfide bridge 308 may be formed between the two sulfur atoms. Such disulfide bridges may close the crack 304 and bring the electrode surface back to original or near-original conformation. Therefore, the SMPU in the shape-memory layers 202, 204 may provide self-regeneration properties to the positive electrode 102 and the negative electrode 104, respectively.

[031] Referring back to FIG. 2, the separator 106 may be a permeable membrane fabricated using at least one material selected from a group including fluorinated polyimmide, polyacrylonitrile (PAN) fiber, decabromodiphenyl ethane, and boron nitride. In an embodiment, the separator 106 may be fabricated using at least one material selected from a group including fluorinated polyimmide at a concentration of about 0.1 M with PAN fibers at a concentration of about 0.5 mM, decabromodiphenyl ethane at a concentration of about 0.5 mM, and functional layers of boron nitride at a concentration of about 0.1mM. It may be noted that the separator 106 may be configured to provide thermal insulation.

[032] Further, the self-regenerating lithium battery 200 may include an electrolyte disposed through the separator 106 and in contact with each of the positive electrode 102 and the negative electrode 104. It may be noted that the electrolyte is configured to rectify one or more anomalies in the self-regenerating lithium battery 200. By way of an example, the one or

more anomalies may include, but may not be limited to, cracks in the electrolyte and cracks in at least one of the positive electrode 102 and the negative electrode 104. The electrolyte may include ethylene carbonate (EC), diethylene carbonate (DEC), and a solution of Gallium-Tin-Barbituric acid (GTB)-Lithium hexafluorophosphate ($LiPF_6$). In an embodiment, the electrolyte may include EC and DEC in a ratio of about 1:1 (v/v) and the GTB-$LiPF_6$ solution at a concentration in a range of about 5% to about 50% by volume. The GTB-$LiPF_6$ solution may include Gallium-Tin alloy and barbituric acid in a mass ratio of about 5:2 dissolved in 1.0 M $LiPF_6$. The GTB is configured to provide hydrogen bonds and electrostatic bonds to rectify the one or more anomalies.

[033] In an embodiment, the electrolyte may be prepared through a process including mixing Gallium-Tin alloy with about 0.02% sodium dodecyl sulfate (SDS) by weight and acetonitrile to obtain a Gallium-Tin suspension. Further, the electrolyte preparation process may include subjecting the Gallium-Tin suspension to ultrasonication to obtain Gallium-Tin suspension droplets. Further, the electrolyte preparation process may include adding barbituric acid to the Gallium-Tin suspension droplets in a mass ratio of about 5:2 to obtain a GTB slurry. Further, the electrolyte preparation process may include coating a nanofilm of the GTB slurry on a carbon cloth through Metal Organic Chemical Vapor Deposition (MOCVD). Thickness of the nanofilm may be in a range of about 500 pm to about 5 nm. Further, the electrolyte preparation process may include grinding the nanofilm-coated carbon cloth using a ball mill to obtain a GTB powder. Size of GTB powder crystals may be in a range of about 1 nm to about 5 nm. Further, the electrolyte preparation process may include dissolving the GTB powder in 1.0 M $LiPF_6$ to obtain the GTB-$LiPF_6$ solution.

[034] Referring now to FIG. 4, rectification of a crack 402 in an exemplary electrolyte 404 of a lithium-ion battery 406 is illustrated, in accordance with some embodiments. The lithium-ion battery 406 may be analogous to the self-regenerating lithium-ion battery 200. The crack 402 may be formed in the electrolyte 404 due to overcharging or overheating. The electrolyte 404 may include EC, DEC, and GTB-$LiPF_6$ solution. The GTB-$LiPF_6$ solution may include Gallium-Tin alloy and barbituric acid in a mass ratio of about 5:2 dissolved in 1.0 M $LiPF_6$.

[035] Further, GTB may be organized as a hybrid metal-organic framework 408 that provides hydrogen bonds and electrostatic interactions. When the crack 402 is formed, molecules of the electrolyte may be separated due to the crack. The hydrogen bonds and electrostatic interactions may bring molecules of the electrolyte closer to each other thereby

narrowing the crack 402 and may eventually close the crack 402 and bring the electrolyte back to original or near-original conformation. Therefore, the GTB in the GTB-$LiPF_6$ solution may provide self-regeneration properties to the electrolyte.

[036] Referring to FIG. 2, a magnetic sensor film 206 may be coated on the surface of the positive electrode 102 and a magnetic sensor film 208 may be coated on the surface of the negative electrode 104. The magnetic sensor film 206 and the magnetic sensor film 208 may be configured to monitor a plurality of battery health parameters corresponding to the positive electrode 102 and the negative electrode 104, respectively. Each of the magnetic sensor films 206 and 208 may monitor the plurality of battery health parameters by monitoring a change in current. Each of the magnetic sensor films 206 and 208, may include one-atom-thick film of a plurality of buckled graphdiyne-carbon nitride QNs coated on flexible ceramic fibers.

[037] A process to develop the magnetic sensor films 206 and 208 may require development of a graphdiyne-carbon nitride film and imprinted polymeric QNs. The graphdiyne-carbon nitride film may be developed on ceramic fiber surface by metal organic chemical vapour deposition. In an embodiment, the graphdiyne and carbon nitride (at a ratio of about 3M:1M) was dissolved in dimethyl sulfoxide (DMSO) and then dried for 50 hours at 65°C. The resultant solid was pulvenrized prior to pyrolysis to obtain thin films. The thin films were deposited onto cleaned flexible ceramic fiber substrates with thickness of about 5 nm to about 100 mm at about 540˚C for about 1.5 hours using nitrogen as a carrier gas with flow rate of about 2.0 dm^3/min to obtain a graphdiyne-carbon nitride monolayer. The developed graphdiyne-carbon nitride monolayer (about 0.2 nm – 3 nm thickness) may not be affected by presence of in-plane stray electromagnetic fields that may severely impact on accuracy of alternative sensing mechanisms.

[038] The imprinted polymeric QNs may be synthesized by providing an imprinted memory to a plurality of buckled graphdiyne-carbon nitride QNs using molecular imprinting technology. The imprinted memory enables recognition of one or more compounds produced due to the one or more anomalies, by the buckled graphdiyne-carbon nitride QNs. About 15 mL of Graphene QNs (about 3 mg in 10 mL) were added along with sodium (0.5 mg) and calcium nanoparticles (0.5mg) in a flask. The imprinted memory allows good spatial resolution and magnetic measurement of a target compound in small spaces. Further, about 50 µL of Aminopropyltriethoxysilane (APTES) was added and stirred for about 2-3 hours under vigorous stirring to allow the APTES to self-assemble onto the Graphene QNs doped with calcium and sodium nanoparticles. A template (for example, H_2 in form of metal hydride, CO,

CO_2 (carbonates), methane (iodoform/chloroform), and volatile organic compounds) corresponding to the target compound to be detected was then dissolved in about 10 mL of ultrapure water and added to the Graphene QNs solution. After stirring for about 15 min, 100 µL of ammonium hydroxide solution (about 35%) was added, and then about 100 µL of TEOS and about 15 mL of ethanol were added drop by drop. The reaction mixture was stirred at room temperature for about 32 hours to obtain Graphene QNs-Molecular Imprinted Polymers (GQNs-MIPs). The GQNs-MIPs were collected by centrifugation, and then washed thoroughly with ethanol and MilliQ water. After each washing step, the supernatant was measured by UV spectrometry to check for template residue in the GQNs-MIPs solution. Further, the process may include forming the one-atom-thick film of the memory imprinted buckled graphdiyne-carbon nitride QNs using spin coating. A solution of imprinted quantum film in ethanol was spin coated on the graphdiyne-carbon nitride film. Further, the process may include directing the spin coated one-atom-thick film of the buckled graphdiyne-carbon nitride QNs on the flexible ceramic fibers using wafer technology. About 20 mg/mL molecular imprinted QNs was mixed with oleic acid in chloroform and spin coated at 2500 rpm for about 10 seconds – 20 seconds. The spin coated film was dried under nitrogen on a hot plate for about 30 minutes at about 80 °C. A dense magnetic sensor film was obtained with a thickness of about 0.5 nm – 10 nm with no cracks. The developed magnetic sensor films 206 and 208 may sense gases (such as, H_2, CO, CH_4, CO_2, and VOCs) in a range of about 10 parts per billion (ppb) to about 500 pg/µL due to imprinted memory.

[039] The magnetic sensor films 206 and 208 are based on Quantum Hall effect, where electrons in a 2-dimensional (2D) material, when subjected to a magnetic field at very low temperature, follow cyclotron orbits with a radius inversely proportional to intensity of the magnetic field. Further, when magnetic sensor films 206 and 208 are subjected to a perpendicular magnetic field and a perpendicular current flow, Lorenz force perpendicular to the magnetic field and current flow may be developed. The Lorenz force further generates an electric field due to development of voltage at the separation of positive and negative charge carrier on surface of the magnetic sensor films 206 and 208.

[040] Therefore, the magnetic sensor films 206 and 208 may monitor the plurality of battery health parameters (for example, electrode cracks, chemical reactions, cell-level electrode deformation, current density mapping, heat generation, battery chemistry, or the like) in a dual mode. Firstly, the magnetic sensor films 206 and 208 may monitor the plurality of battery health parameters by monitoring a change in current produced as a result of one or more

anomalies (for example, cracks in an electrode or electrolyte). Secondly, the magnetic sensor films 206 and 208 may monitor the plurality of battery health parameters by detecting presence and/or concentration of various gases that may be released as a result of the one or more anomalies.

[041] In addition to monitoring one or more anomalies, the magnetic sensor films 206 and 208 may monitor rectification of the one or more anomalies through the plurality of battery health parameters. For example, if there is a fluctuation in current flow due to the presence of one or more anomalies, the same fluctuation may reduce and eventually the current flow may return to original or near-original values upon rectification of the one or more anomalies. Similarly, if there is a rise in concentration of a gas indicating presence of one or more anomalies, the same gas concentration may reduce and eventually return to original or near-original values upon rectification of the one or more anomalies. It should be noted that the ceramic fibers used in the magnetic sensor films 206 and 208 are flexible like cloth and are also heat resistant to withstand higher temperatures during battery operation. Thus, the magnetic sensor films 206 and 208 may be integrated in any type of battery form or design (e.g., pouch, prismatic, cylindrical, etc.).

[042] It should be noted that the lithium-ion battery 200 can give high specific capacity of about 700.8 mAh g^{-1} at about 0.1 A g^{-1} and a high rate capability at about 3 A g^{-1} (400.4 mAh g^{-1}, 80% of the initial capacity) at a temperature in a range of about -10 °C to about 200 °C. Moreover, the QNs at the negative electrode 104 also show a stable capacity retention of about 95.1% at about 1 A g–1 after stabilizing cycles (from about 100 to about 2000 cycles).

[043] In some embodiments, the lithium-ion battery 200 may generate a voltage of about 3.8 to about 4.0 volts (V). Further, the lithium-ion battery 200 may provide a specific energy (capacity) of about 800 to about 1,000 kWh/kg. Further, the lithium-ion battery 200 may include a charge (c-rate) of about 1C (typical) to about 5C (maximum) and may charge to 3.0V. Further, for the lithium-ion battery 200, a discharge (c-rate) of about 10C may be possible, with about 30C 5s pulse and about 1.80V cut-off. Further, a cycle life of the lithium-ion battery 200 may be 10,000–20,000 cycles and a thermal runaway of temperatures as high as about 400 °C to about 500 °C and as low as about 0 °C to about -40 °C.

[044] Referring now to FIG. 5, an exemplary method 500 for assembling a self-regenerating lithium-ion battery (such as, the self-regenerating lithium-ion battery 200) is depicted via a flow chart, in accordance with some embodiments. The method 500 may include

electrically coupling a positive electrode (such as, the positive electrode 102) with a negative electrode (such as, the negative electrode 102), at step 502. Each of the positive electrode and the negative electrode may include QNs doped in SMPU. The SMPU may regenerate using shape-memory effect and disulfide exchange reaction.

[045] Further, the method 500 may include coating a magnetic sensor film (such as, the magnetic sensor films 206 and 208) on each of the positive electrode and the negative electrode, at step 504. The magnetic sensor film may monitor a plurality of health parameters by monitoring a change in current flowing through the electrically coupled positive electrode and negative electrode. By way of an example, the plurality of battery health parameters may include electrode cracks, chemical reactions, cell-level electrode deformation, current density mapping, and heat generation. The magnetic sensor film may include molecular imprinted polymers that provide an imprinted memory to the magnetic sensor film. In some embodiments, the magnetic sensor film may be configured to detect a plurality of gases released from the electrode using the imprinted memory. Further, the magnetic sensor film may monitor a change in current due to fluctuations in voltage induced by a change in at least one of the plurality of battery health parameters through Quantum Hall effect.

[046] In an embodiment, the magnetic sensor film may include one-atom-thick film of a plurality of buckled graphdiyne-carbon nitride QNs coated on flexible ceramic fibers. The magnetic sensor film may be developed by providing an imprinted memory to a plurality of buckled graphdiyne-carbon nitride QNs using molecular imprinting technology. The imprinted memory may enable recognition of one or more compounds produced due to the one or more anomalies, by the buckled graphdiyne-carbon nitride QNs. Further, developing the magnetic sensor film may include forming the one-atom-thick film of the memory imprinted buckled graphdiyne-carbon nitride QNs using spin coating. Further, developing the magnetic sensor film may include directing the one-atom-thick film of the buckled graphdiyne-carbon nitride QNs on the flexible ceramic fibers using wafer technology.

[047] Further, the method 500 may include disposing each of the positive electrode and the negative electrode in contact with an electrolyte, at step 506. The electrolyte may be configured to rectify one or more anomalies. The one or more anomalies may be detected based on at least one of the plurality of battery health parameters. The electrolyte may include at least one of EC, DEC, and a solution of GTB- $LiPF_6$.

[048] Further, the method 500 may include positioning a separator (such as, the separator 106) between the positive electrode and the negative electrode, at step 508. The

separator may be configured to provide thermal insulation. The separator may be fabricated using at least one material selected from a group comprising of fluorinated polyimmide, polyacrylonitrile (PAN) fiber, decabromodiphenyl ethane, and boron nitride.

[049] Referring now to FIG. 6, Scanning Electron Microscopy (SEM) images depicting self-regeneration of an exemplary electrolyte are illustrated, in accordance with some embodiments. In an SEM image 600A, an original conformation of the electrolyte is observed prior to lithiation. There are no signs of a crack in the electrode surface at this point of time. In SEM image 600B, structure of the electrolyte after crack formation upon lithiation is observed. The crack appears as a dark region indicating formation of a gap in the electrolyte sample. In SEM image 600C, self-healing at 2 seconds after crack formation is observed. The crack is starting to rectify at 2 seconds as the gap has narrowed down. In SEM image 600D, self-healing of the electrolyte at 15 seconds after crack formation is observed. The electrolyte has attained the original or near-original conformation at 15 seconds as the gap has completely disappeared. This is due to formation of metal-ligand co-ordination bonds and hydrogen bonds in electrolyte.

[050] In an exemplary embodiment, as per FIG. 7, a table 700 representing self-regenerating properties of various electrolytes is illustrated. The table 700 includes data corresponding to electrolyte, filler used in the electrolyte, filler content percentage, and various self-regenerating properties of the electrolyte namely, conductivity, self-healing time, and mechanical strength.

[051] When EC/DEC is used as the electrolyte and Gallium-Tin nanomaterials (200 nm – 500 nm in size) are used as filler at a filler content percentage of 5% - 15%, the conductivity is 5.6×10^5 to 6.5×10^5, the self-healing time is 150 minutes to 200 minutes, and the mechanical strength is 68 KPa.

[052] When EC/DEC is used as the electrolyte and Gallium-Tin nanomaterials (1 pm – 100 nm in size) are used as filler at a filler content percentage of 5%, the conductivity is 7.5×10^5, the self-healing time is 90 minutes, and the mechanical strength is 95 KPa.

[053] When EC/DEC is used as the electrolyte and barbituric acid is used as filler at a filler content percentage of 10%, the conductivity is 9.4×10^5, the self-healing time is 102 minutes, and the mechanical strength is 87 KPa.

[054] When EC/DEC is used as the electrolyte and Gallium-Tin nanomaterials (1 pm – 100 nm in size)-barbituric acid (GTB) film is used as filler at a filler content percentage of 5% - 10%, the conductivity is 10.2×10^5, the self-healing time is 0.1 minutes to 10 minutes, and the mechanical strength is 130 KPa.

[055] Therefore, GTB as a filler material enhances the self-regeneration capacity of the electrolyte by providing an increased conductivity, lowering the self-healing time, and improving the mechanical strength of the electrolyte.

[056] It should be noted that the table 700 is an exemplary embodiment only and is based on laboratory-scale experiments corresponding to that particular embodiment. Data provided in the table 700 is intended to provide support to the claims and is not limiting to the overall scope of the invention.

[057] In an exemplary embodiment, as per FIG. 8, a graph 800 representing self-regeneration percentages of various electrolytes is illustrated. Y-axis of the graph 800 represents self-healing percentage and X-axis of the graph 800 represents time. The self-healing percentage implies percentage of a crack in an electrolyte that is now rectified. As per the graph 800, EC-DEC-GTB electrolyte achieves maximum self-healing percentage in least time as compared to EC-DEC-BA, EC-DEC-GT Quantum particles, EC-DEC-GT nanoparticles, and EC-DEC (i.e., control). This confirms the data provided by the table 700 with respect to enhanced self-regeneration properties of GTB filler along with EC-DEC electrolyte.

[058] It should be noted that the graph 800 is an exemplary embodiment only and is based on laboratory-scale experiments corresponding to that particular embodiment. Data provided in the graph 800 is intended to provide support to the claims and is not limiting to the overall scope of the invention.

[059] Tests were conducted on different electrolyte samples by a continuous dynamic flexural deformation. The electrolyte samples ($1\times 1 \times 10$ mm^3) and a V-shaped starter notch, (1×1 mm^2) were analyzed by applying a sinusoidal deformation with a maximum amplitude of 0.1% at a frequency of 5 Hz. A pre-crack in each of the electrolyte samples was induced by an impulsive load of about 10 N. Further, evolution of mechanical modulus with time was considered as representative of evolution of healing process in the electrolyte sample. Self-healing efficiency of the electrolyte samples was analyzed. The self-healing efficiency may be defined as a ratio between an actual elastic modulus (E') during measurement and an elastic modulus of a pristine electrolyte sample (E') before applying the crack.

[060] All the samples containing modified EC/DEC show partial recovery of the elastic modulus during monitoring. The pattern is quite similar for all formulations. After an initial delay, the recovery mechanism is indicated by a rise of the elastic modulus up to a maximum and a subsequent reduction of the self-healing efficiency. The EC-DEC electrolyte

sample did not show any self-healing, indicating that EC/DEC alone may be unable to confer a self-healing functionality to the electrolyte. The EC-DEC-GTB electrolyte sample showed highest self-healing efficiency with time due to GTB quantum properties and an outstanding efficiency to cross-link the electrolyte again via hydrogen bonds and metal-ligand coordination bonds with GTB molecules in EC-DEC electrolytes.

[061] Thus, the disclosed self-regenerating lithium-metal ion battery tries to overcome the technical problem of providing lithium-ion batteries with electrodes and electrolytes capable of self-regeneration. The electrodes of the lithium-ion battery include SMPU that enables regeneration of electrodes in case of any anomalies and the electrolyte of the lithium-ion battery includes GTB that provides a hybrid metal organic framework which helps in healing the anomalies within 15 seconds by providing hydrogen bonds and transition metal coordination bonds. The self-regeneration abilities of the electrodes and the electrolyte may enhance cycle life of the lithium-ion battery to about 10,000–20,000 cycles. The lithium-ion battery may include a thermal runaway of temperatures as high as about 400 °C to about 500 °C and as low as about 0 °C to about -40 °C making it one of the safest lithium-ion batteries. Further, the lithium-ion battery includes magnetic sensor films that function based on Quantum Hall effect. The magnetic sensor films can detect gases leaking because of the anomalies at a concentration as low as 10 ppb. The magnetic sensor films are also capable of detecting fluctuation in current due to the anomalies. Thus, the dual function magnetic sensor films can detect anomalies in the battery at early stages and also detect healing or rectification the anomalies after the self-regeneration. Thus, the lithium-ion battery has an enhanced life as the electrodes and electrolytes have self-healing and self-regeneration properties that allow the battery to overcome deformation and structural anomalies over multiple charging cycles.

[062] As will be appreciated by those skilled in the art, the techniques described in the various embodiments discussed above are not routine, or conventional, or well understood in the art. The techniques discussed above provide for assembling a self-regenerating lithium-ion battery. The techniques may first electrically couple a positive electrode with a negative electrode. Each of the positive electrode and the negative electrode includes QNs doped in SMPU. The SMPU regenerates using shape-memory effect and disulfide exchange reaction. The techniques may then coat a magnetic sensor film on each of the positive electrode and the negative electrode. The magnetic sensor film monitors a plurality of health parameters by monitoring a change in current. The techniques may then dispose each of the positive electrode and the negative electrode in contact with an electrolyte. The electrolyte is configured to rectify

one or more anomalies. The one or more anomalies are detected based on at least one of the plurality of battery health parameters. The electrolyte includes at least one of EC, DEC, and a solution of GTB- $LiPF_6$.

[063] In light of the above-mentioned advantages and the technical advancements provided by the disclosed method and system, the claimed steps as discussed above are not routine, conventional, or well understood in the art, as the claimed steps enable the following solutions to the existing problems in conventional technologies. Further, the claimed steps clearly bring an improvement in the functioning of the device itself as the claimed steps provide a technical solution to a technical problem.

[064] The specification has described a self-regenerating lithium-ion battery, a method of assembling the self-regenerating lithium-ion battery, and a magnetic sensor film to monitor battery health parameters of the same. The illustrated steps are set out to explain the exemplary embodiments shown, and it should be anticipated that ongoing technological development will change the manner in which particular functions are performed. These examples are presented herein for purposes of illustration, and not limitation. Further, the boundaries of the functional building blocks have been arbitrarily defined herein for the convenience of the description. Alternative boundaries can be defined so long as the specified functions and relationships thereof are appropriately performed. Alternatives (including equivalents, extensions, variations, deviations, etc., of those described herein) will be apparent to persons skilled in the relevant art(s) based on the teachings contained herein. Such alternatives fall within the scope and spirit of the disclosed embodiments.

[065] It is intended that the disclosure and examples be considered as exemplary only, with a true scope and spirit of disclosed embodiments being indicated by the following claims.

WE CLAIM:

1. A lithium-ion battery (200) comprising:

a positive electrode (102) and a negative electrode (104), wherein each of the positive electrode (102) and the negative electrode (104) comprises Quantum Nanomaterials (QNs) doped in shape-memory polyurethane (SMPU), and wherein the SMPU regenerates using shape-memory effect and disulfide exchange reaction;

a magnetic sensor film coated on each of the positive electrode (102) and the negative electrode (104), wherein the magnetic sensor film monitors a plurality of battery health parameters by monitoring a change in current, and wherein the magnetic sensor film comprises one-atom-thick film of a plurality of buckled graphdiyne-carbon nitride QNs coated on flexible ceramic fibers; and

an electrolyte in contact with each of the positive electrode (102) and the negative electrode (104), wherein the electrolyte is configured to rectify one or more anomalies, wherein the one or more anomalies are detected based on at least one of the plurality of battery health parameters, and wherein the electrolyte comprises at least one of: ethylene carbonate (EC), diethylene carbonate (DEC), and a solution of Gallium-Tin-Barbituric acid (GTB)-Lithium hexafluorophosphate ($LiPF_6$).

2. The lithium-ion battery (200) as claimed in claim 1, further comprising a separator positioned between the positive electrode (102) and the negative electrode (104), wherein the separator is configured to provide thermal insulation, wherein the separator is fabricated using at least one material selected from a group comprising of fluorinated polyimmide, polyacrylonitrile (PAN) fiber, decabromodiphenyl ethane, and boron nitride.

3. The lithium-ion battery (200) as claimed in claim 1, wherein the magnetic sensor film is coated on each of the positive electrode (102) and the negative electrode (104) based on molecular imprinting technology to provide an imprinted memory to buckled graphdiyne-carbon nitride QNs, wherein the imprinted memory enables recognition of one or more compounds produced due to the one or more anomalies, by the buckled graphdiyne-carbon nitride QNs, wherein the one-atom-thick film of the memory imprinted buckled graphdiyne-carbon nitride QNs is provided using spin coating, and wherein the one-atom-thick film of the buckled graphdiyne-carbon nitride QNs is directed on the flexible ceramic fibers using wafer technology.

4. The lithium-ion battery (200) as claimed in claim 1, wherein the plurality of battery health parameters comprises electrode cracks, chemical reactions, cell-level electrode deformation, current density mapping, and heat generation.

5. The lithium-ion battery (200) as claimed in claim 1, wherein the monitoring of the plurality of battery health parameters is based on at least one of:

detection of a plurality of gases released from at least one of the positive electrode (102) and the negative electrode (104) using the imprinted memory, wherein concentration of each of the plurality of gases is at least 10 parts per billion (ppb); and

the change in current monitored due to fluctuations in voltage induced by a change in at least one of the plurality of battery health parameters through Quantum Hall effect.

6. A method of assembling a lithium-ion battery (200), the method comprising:

electrically coupling a positive electrode (102) with a negative electrode (104), wherein each of the positive electrode (102) and the negative electrode (104) comprises Quantum Nanomaterials (QNs) doped in Shape-Memory Polyurethane (SMPU), and wherein the SMPU regenerates using shape-memory effect and disulfide exchange reaction;

coating a magnetic sensor film on each of the positive electrode (102) and the negative electrode (104), wherein the magnetic sensor film monitors a plurality of health parameters by monitoring a change in current; and

disposing each of the positive electrode (102) and the negative electrode (104) in contact with an electrolyte, wherein the electrolyte is configured to rectify one or more anomalies, wherein the one or more anomalies are detected based on at least one of the plurality of battery health parameters, and wherein the electrolyte comprises at least one of ethylene carbonate (EC), diethylene carbonate (DEC), and a solution of Gallium-Tin-Barbituric acid (GTB)-Lithium hexafluorophosphate ($LiPF_6$).

7. The method as claimed in claim 6, further comprising positioning a separator between the positive electrode (102) and the negative electrode (104), wherein the separator is configured to provide thermal insulation, wherein the separator is fabricated using at least one material selected from a group comprising of fluorinated polyimmide, polyacrylonitrile (PAN) fiber, decabromodiphenyl ethane, and boron nitride.

8. The method as claimed in claim 6, wherein the magnetic sensor film comprises one-atom-thick film of a plurality of buckled graphdiyne-carbon nitride QNs coated on flexible ceramic fibers, and wherein the magnetic sensor film is developed by:

providing an imprinted memory to a plurality of buckled graphdiyne-carbon nitride QNs using molecular imprinting technology, wherein the imprinted memory enables recognition of one or more compounds produced due to the one or more anomalies, by the buckled graphdiyne-carbon nitride QNs;

forming the one-atom-thick film of the memory imprinted buckled graphdiyne-carbon nitride QNs using spin coating; and

directing the one-atom-thick film of the buckled graphdiyne-carbon nitride QNs on the flexible ceramic fibers using wafer technology.

9. A magnetic sensor film for monitoring a plurality of battery health parameters of an electrode, the magnetic sensor film comprising:

a layer of flexible ceramic fibers.

one-atom-thick film of a plurality of buckled graphdiyne-carbon nitride Quantum Nanomaterials (QNs) coated on the layer of flexible ceramic fibers using wafer technology, wherein the buckled graphdiyne-carbon nitride QNs comprises an imprinted memory provided by molecular imprinting, wherein the one-atom-thick film of the buckled graphdiyne-carbon nitride QNs is formed using spin coating, and wherein the imprinted memory enables recognition of one or more compounds produced due to one or more anomalies detected based on at least one of the plurality of battery health parameters.

10. The magnetic sensor film as claimed in claim 9, configured to, at least one of:

detect a plurality of gases released from the electrode using the imprinted memory; and

monitor a change in current due to fluctuations in voltage induced by a change in at least one of the plurality of battery health parameters through Quantum Hall effect.

Dated this 14th day of November 2022

-- Digitally Signed--
Bhanu Prasad
(INPA No: **3253**)
Manager, IPR Dept.,
L&T Technology Services Limited,
DLF 3rd Block, 2nd Floor,
Manapakkam, Chennai - 600089.

ABSTRACT

SELF-REGENERATING LITHIUM-ION BATTERY

This disclosure relates to a self-regenerating lithium-ion battery (200). The lithium-ion battery (200) includes a positive electrode (102) and a negative electrode (104). Each of the positive electrode (102) and the negative electrode (104) includes Quantum Nanomaterials (QNs) doped in shape-memory polyurethane (SMPU). The lithium-ion battery (200) further includes a magnetic sensor film coated on each of the positive electrode (102) and the negative electrode (104). The magnetic sensor film monitors a plurality of battery health parameters by monitoring a change in current. The magnetic sensor film includes one-atom-thick film of a plurality of buckled graphdiyne-carbon nitride QNs coated on flexible ceramic fibers. The lithium-ion battery (200) further includes an electrolyte in contact with each of the positive electrode (102) and the negative electrode (104). The electrolyte is configured to rectify one or more anomalies detected based on at least one of the plurality of battery health parameters.

[To be published with FIG. 2]

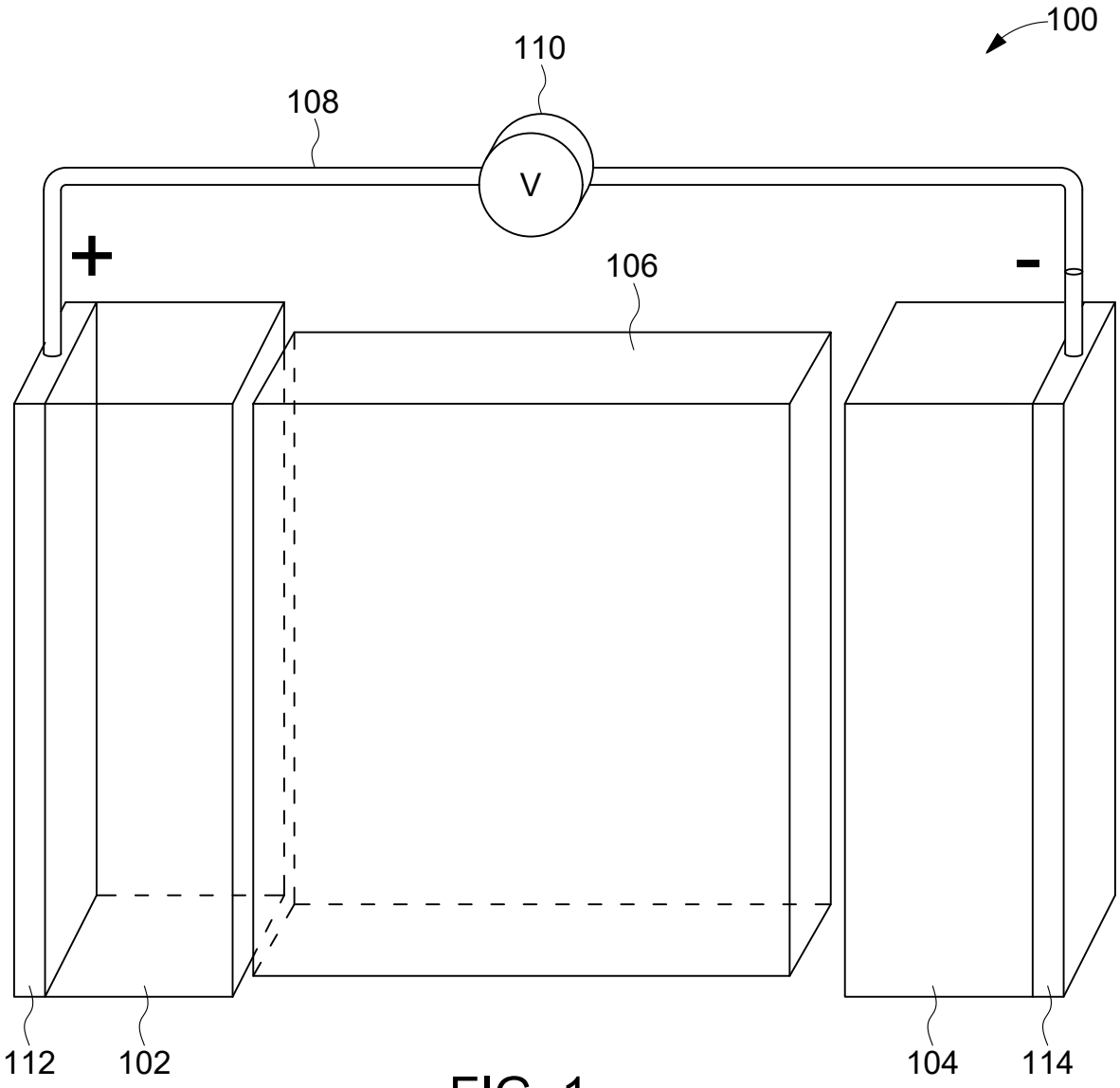

FIG. 1

-- Digitally Signed--
Bhanu Prasad
(INPA No: 3253)
Manager, IPR Dept.,
L&T Technology Services Limited,
DLF 3rd Block, 2nd Floor,
Manapakkam, Chennai - 600089.

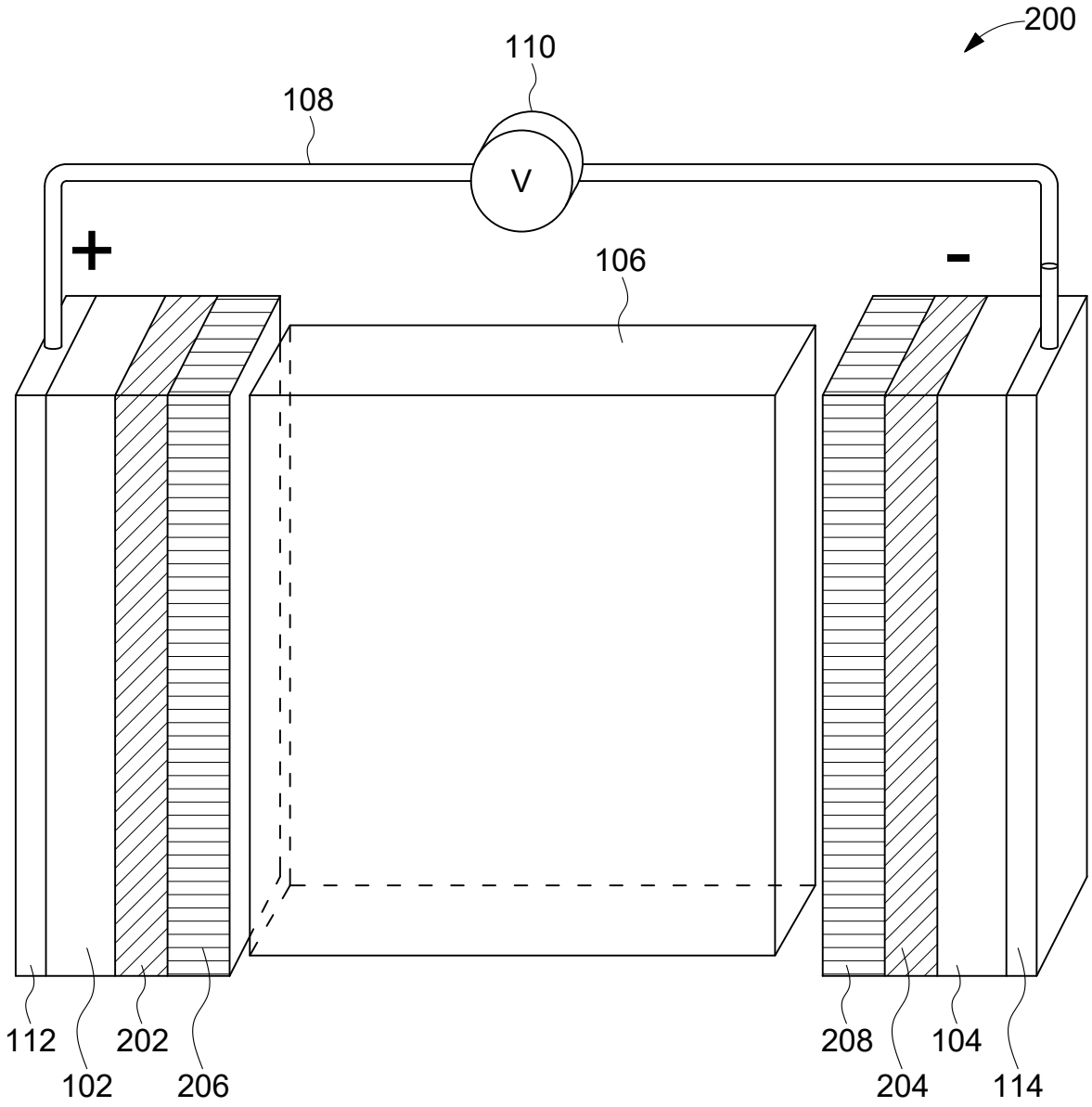

FIG. 2

-- Digitally Signed--
Bhanu Prasad
(INPA No: 3253)
Manager, IPR Dept.,
L&T Technology Services Limited,
DLF 3rd Block, 2nd Floor,
Manapakkam, Chennai - 600089.

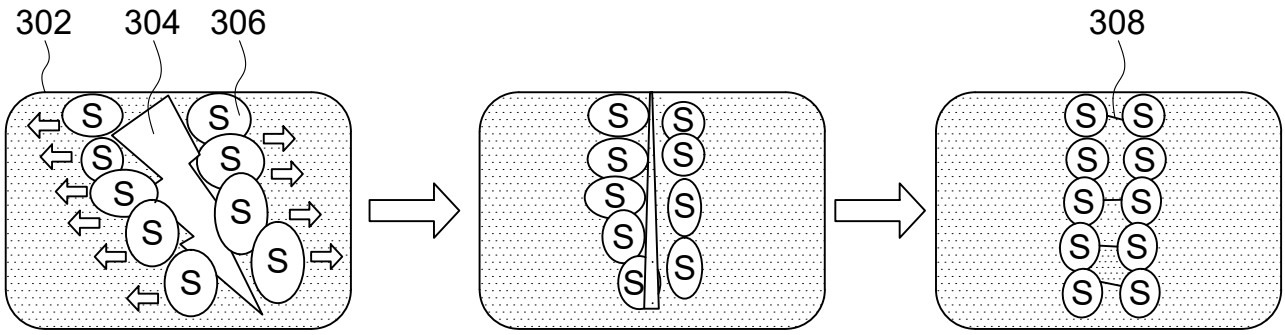

FIG. 3

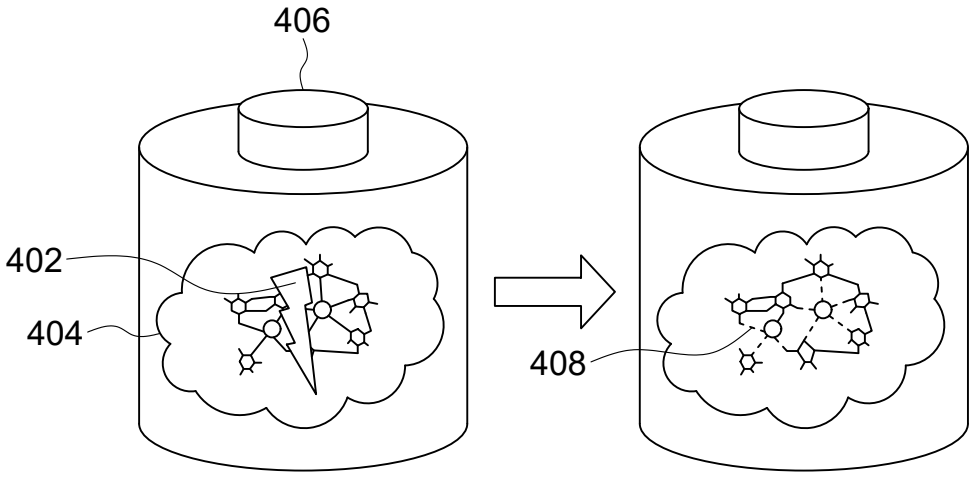

FIG. 4

-- Digitally Signed--
Bhanu Prasad
(INPA No: 3253)
Manager, IPR Dept.,
L&T Technology Services Limited,
DLF 3rd Block, 2nd Floor,
Manapakkam, Chennai - 600089.

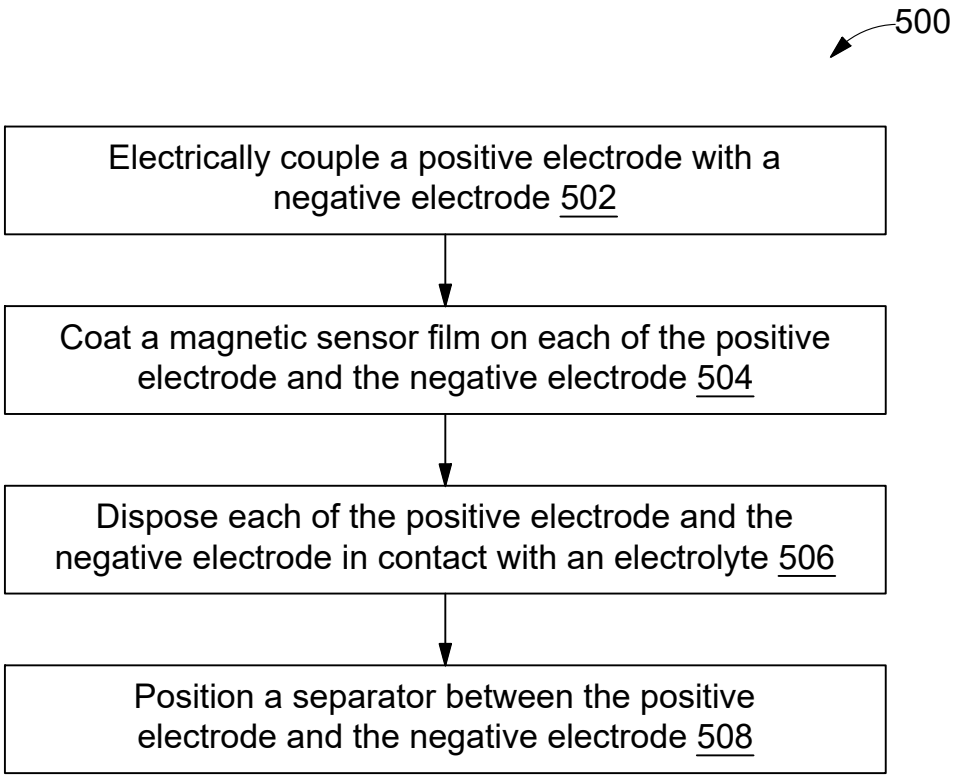

FIG. 5

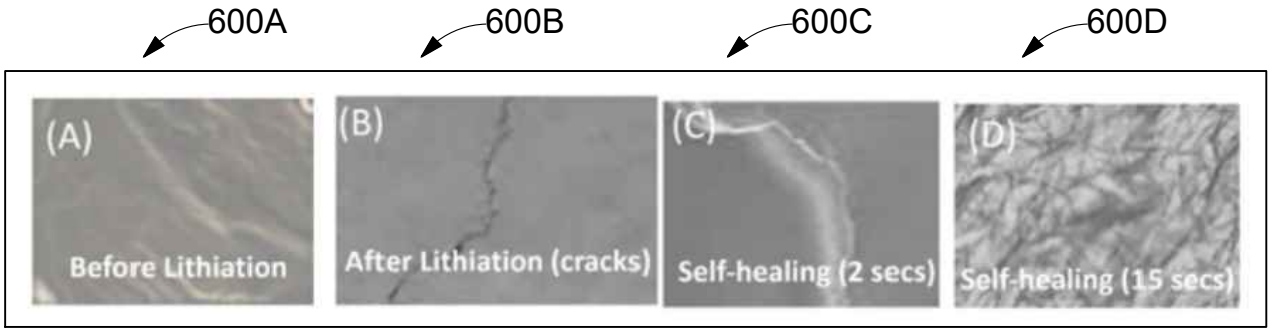

FIG. 6

-- Digitally Signed--
Bhanu Prasad
(INPA No: 3253)
Manager, IPR Dept.,
L&T Technology Services Limited,
DLF 3rd Block, 2nd Floor,
Manapakkam, Chennai - 600089.

700

S.No	Electrolyte	Filter	Filter Content %	Conductivity (S cm-1) at 35°C	Self-healing time (min)	Mechanical Strength (Kpa)
1.	EC/DEC	Gallium-Tin nanomaterials (200-500 nm)	5-15	$5.6x10^5$ to $6.5x10^5$	150-200	68
2.	EC/DEC	Gallium-Tin nanomaterials (1 pico-100 nm)	5	$7.5x10^5$	90	95
3.	EC/DC	Barbituric acid	10	$9.4x10^5$	102	87
4.	EC/DC	Gallium-Tin nanomaterials (1 pico-100 nm)-Barbituric acid film (GTB)	5-10	$10.2x10^5$	0.1-10	130

FIG. 7

-- Digitally Signed--
Bhanu Prasad
(INPA No: 3253)
Manager, IPR Dept.,
L&T Technology Services Limited,
DLF 3rd Block, 2nd Floor,
Manapakkam, Chennai - 600089.

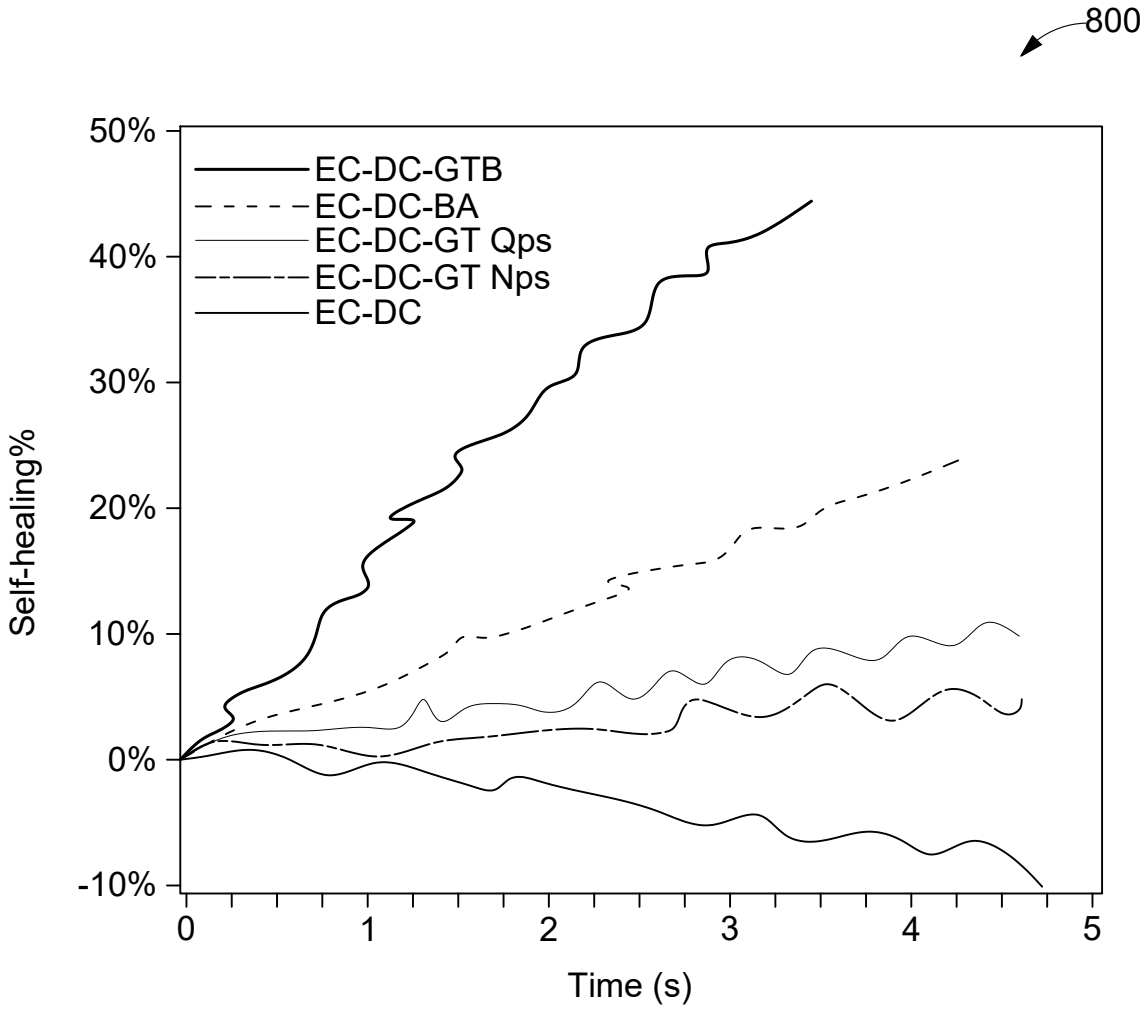

FIG. 8

-- Digitally Signed--
Bhanu Prasad
(INPA No: 3253)
Manager, IPR Dept.,
L&T Technology Services Limited,
DLF 3rd Block, 2nd Floor,
Manapakkam, Chennai - 600089.